

# Frequency doubling of 1560nm diode laser via PPLN and PPKTP crystals and frequency stabilization to rubidium absorption line

Shanlong Guo, Jianfeng Yang, Baodong Yang, Tiancai Zhang, and Junmin Wang \*  
State Key Laboratory of Quantum Optics and Quantum Optics Devices,  
and Institute of Opto-Electronics, Shanxi University,  
No. 92 Wucheng Road, Taiyuan 030006, Shanxi Province, P. R. China

## ABSTRACT

In our experiment, a polarization-maintaining (PM) fiber-pigtailed butterfly-sealed 1560nm distributed-feedback (DFB) laser diode is amplified by a 5-Watt EDFA, then a multiple-period PPLN crystal (1mm×10mm×20mm) and a single-period PPKTP crystal (1mm×2mm×30mm) are utilized to perform SHG via single pass configuration. The second harmonic power of ~ 239 mW@780 nm for PPLN and ~ 210 mW@780 nm for PPKTP are obtained with ~5W@1560 nm laser input, corresponding to SHG efficiency of ~ 5.2% for PPLN and ~ 4.4% for PPKTP, respectively. Finally the 1560 nm laser diode's frequency is locked to rubidium absorption line via SHG and rubidium absorption spectroscopy, the laser frequency drift for free-running case is ~ 56 MHz in 30 s, the residual frequency drift after being locked is ~ ± 3.5 MHz.

**Keywords:** DFB diode laser, EDFA, Frequency doubling, PPLN, PPKTP, Quasi phase matching (QPM), Frequency stabilization, Rubidium absorption line

## 1. INTRODUCTION

It is well known that the controlling of the light frequency is important in fundamental research and commercial use, such as the definition of the physical constant, the measurement of the precision spectroscopy and metrology. With the development of the optical communication market, especially the Wavelength Division Multiplexing (WDM) and Dense Wavelength Division Multiplexing (DWDM) system, the technology can be transported multi-beam laser in the same fiber-optical at one time makes the bandwidth of the optical communication magnified. Atomic and molecular absorption line can provide the frequency standard as the calibration of the optical telecommunication channels avoiding cross talk.

Frequency doubling of 1560nm laser diode corresponds to Rb atom D<sub>2</sub> line. Ohtsu *et al* locks 1560-nm laser diode to <sup>87</sup>Rb atom absorption line by using of generated 780-nm optical signal via internal frequency doubling process inside the laser diode <sup>1</sup>. Better 780-nm laser absorption signal with Rb atomic cell will be obtained by utilizing bulk KNbO<sub>3</sub> crystal through external frequency doubling <sup>2</sup>.

Along with Quasi-phase matching (QPM) technology development, higher power at 780 nm will be expected by employing PPLN or PPKTP crystals with higher efficiency of second-harmonic generation (SHG), and finally 1560-nm laser can be easily locked to Rb absorption line <sup>3,4</sup>. Employing 1560-nm laser diode as a master laser, then power amplified by an Er-doped fiber amplifier (EDFA) which is well developed in optical telecommunication field, after frequency doubling via PPLN or PPKTP crystals, one can get higher 780-nm laser power with very good frequency stability (using Rb absorption line as laser frequency reference to lock the master laser). This reliable master-laser plus EDFA and SHG system can be utilized in laser cooling and trapping of Rb atoms especially for exploring the cold atomic clock at aircraft-based weak-gravitation environment <sup>5</sup>.

## 2. EXPERIMENTAL SETUP AND EXPERIMENTAL PRINCIPLE

### 2.1 Experimental setup

The schematic diagram of experimental setup is shown as Fig. 1. Master laser is a PM fiber-pigtailed butterfly-type 1560 nm distributed-feedback (DFB) diode laser. At a temperature of 27 °C and the drive current of 115 mA, this DFB diode laser can generate output power of 14 mW at 1560.50 nm (780.25 nm after SHG). The current tuning coefficient for laser frequency is ~ - 0.49 GHz/mA and the temperature tuning coefficient is ~ -11.2 GHz/°C.

\* *Corresponding author, Email: wwjjmm@sxu.edu.cn, Fax: +86 - 351 - 7011500, Tel: +86 - 351 - 7011844*

In our experiment, one part of the fundamental pump source transmits to confocal Fabry-Perot cavity; another part transmits to EDFA. The half-wave plate placed in front of the EDFA is used to obtain the correct polarization input<sup>6</sup>. The fundamental beam is focused into the SHG crystal using a single lens, with the resulting beam waist positioned at the center of the crystal.

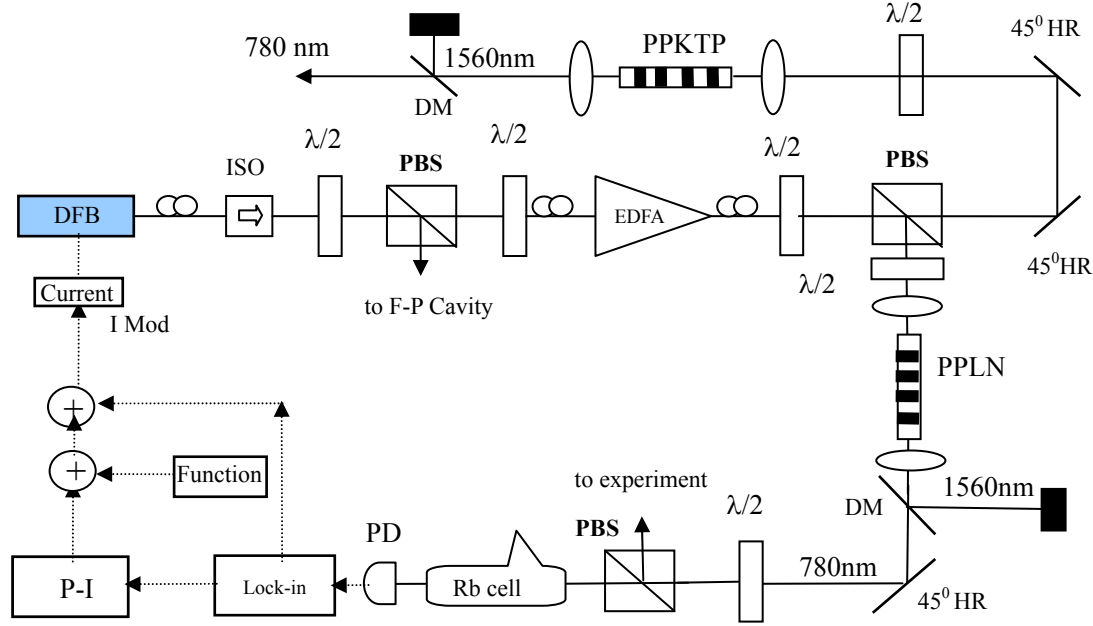


**Fig.1** DFB: distributed-feedback laser diode, ISO: optical isolator, PBS: polarization beamsplitter, EDFA: Er-doped fiber amplifier; PPLN: multiple-period PPLN crystal; PPKTP: single-period PPKTP crystal; P-I: proportion and integration amplifier; DM: dichroic mirror (1560nm HR/780nm HT); Lock-in: lock-in amplifier; I MOD: current modulation port; PD: photodiode. The solid lines indicate the optical routine and the dot lines indicate electronic connection.

The nonlinear crystals used in our experiments are bulk PPKTP and PPLN. Fundamental power is amplified by EDFA, one part of beam is injected to PPKTP crystal, and another part is injected to PPLN crystal. The PPKTP crystal (1mm×2mm×30mm) contains a single period of 24.925 μm; The PPLN crystal (1mm×10mm×20mm) contains six periods of 19.0, 18.8, 18.6, 18.4, 18.2 and 18.0 μm respectively, as shown in Fig. 2. The end faces of the both crystals are antireflection-coated at 1560 nm and 780 nm.

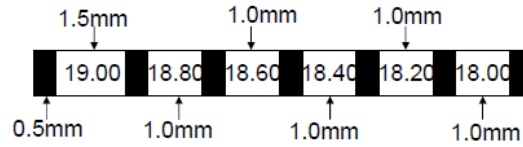


**Fig. 2** Sectional view of PPLN crystal, every blank part corresponds one phase-matching period, unit is μm. The period of 19.0 μm is wider than other periods, and can be regarded as a marker.

## 2.2 Theory for frequency doubling via quasi-phase-matching (QPM) crystal

To the process of QPM, the mismatch of the wave vector can be described by

$$\Delta k = k_2 - 2k_1 - k_m = \frac{2\pi n_2}{\lambda_2} - 2 \cdot \frac{2\pi n_1}{\lambda_1} - \frac{2\pi m}{\Lambda} \quad (1)$$

Where  $n_1$  and  $n_2$  are refractive indices at the fundamental and second harmonic wavelengths,  $\lambda_1$  is the wavelength of fundamental wave in vacuum,  $\lambda_2$  is the wavelength of second harmonic wave in vacuum,  $m$  is the order of QPM, In our

experiment, we adopt the first order QPM ( $m=1$ ),  $\Lambda$  is the QPM period.

According to conservation of momentum and energy, we can get <sup>7</sup>:

$$\Lambda = \frac{m\lambda_1}{2(n_2 - n_1)} \quad (2)$$

The power of the second-harmonic wave reads:

$$P_{2\omega} = \frac{8\pi^2}{c\epsilon_0 n_1^2 n_2 \lambda_1^2} \cdot d_{\text{eff}}^2 \cdot L^2 \cdot \frac{P_{\omega}^2}{\pi w_{10}^2} \cdot \frac{\sin^2(\Delta k L / 2)}{(\Delta k L / 2)^2} \quad (3)$$

The SHG efficiency reads:

$$\eta = \frac{P_{2\omega}}{P_{\omega}} = \frac{8\pi^2}{c\epsilon_0 n_1^2 n_2 \lambda_1^2} \cdot d_{\text{eff}}^2 \cdot L^2 \cdot \frac{P_{\omega}}{\pi w_{10}^2} \cdot \frac{\sin^2(\Delta k L / 2)}{(\Delta k L / 2)^2} \quad (4)$$

where  $P_{\omega}$  is the fundamental power,  $P_{2\omega}$  is second harmonic power,  $c$  is the light speed in vacuum,  $\epsilon_0$  is the dielectric constant of vacuum,  $d_{\text{eff}}$  is the effective nonlinear coefficient,  $L$  is the crystal length,  $w_{10}$  is the Gaussian radius at waist of fundamental wave. When  $\Delta k = 0$ , the final term  $\frac{\sin^2(\Delta k L / 2)}{(\Delta k L / 2)^2} = 1$ . From equation (4), we can see that the SHG

efficiency is affected by  $P_{\omega}$ ,  $w_{10}$  and  $L$ . We selected one of our lenses in hand (the focal length  $f=76, 60, 50, 40$  mm) as the focusing lens for PPLN and PPKTP crystals respectively. Then we find a lens with  $f=76$ mm is suitable for  $1\text{mm} \times 2\text{mm} \times 30\text{mm}$  PPKTP crystal, and a lens with  $f=50$  mm is suitable for  $1\text{mm} \times 10\text{mm} \times 20\text{mm}$  PPLN crystal.

### 3. EXPERIMENTAL RESULTS

#### 3.1 The optimum matching temperature

There is no need to consider the angle in the matching process. By controlling the crystal temperature we can get  $\Delta k=0$  to achieve the best match. Modulation range of the temperature controller is  $40 \sim 200$  °C, controlling precision is  $0.1$  °C. In order to get better temperature control effect, the oven which is consisted of red copper with high heat conductivity encloses the crystal on all sides, except the input and output facets(owing to expansion caused by heat and contraction caused by cold, crystal should no be pressed too tighten). Enclosed oven is the protecting jacket that is processed by heat insulating material polysulfone. Resistance wire is applied to heat in the temperature controller, and the thermistor is used to detect crystal temperature, then feedback information to temperature controller.

In our experiment, we obtained the phase-matching temperature  $113$  °C ( $162$  °C) for the period of  $19.0$   $\mu\text{m}$  ( $18.8$   $\mu\text{m}$ ) for PPLN crystal. The results are shown in Fig. 3.

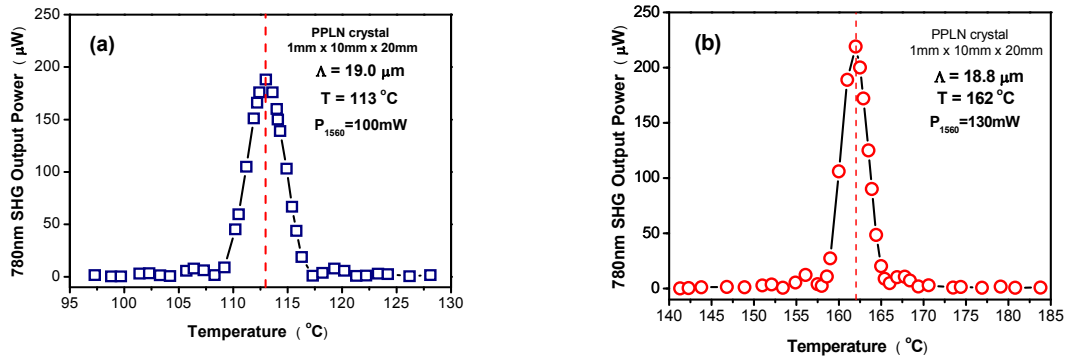


**Fig. 3** (a) Phase matching temperature of period  $19.0 \mu\text{m}$  is  $113$  °C. (b) Phase matching temperature of period  $18.8 \mu\text{m}$  is  $162$  °C. The full-width half-maximum (FWHM) bandwidth  $\Delta T \sim 4$  °C.

Considering photorefractive effect, we apply the matching period  $18.8\mu\text{m}$  in our experiment. Besides, a half-wave plate placed in front of the lens is to regulate polarization of the fundamental wave<sup>8</sup>. In our experiment “s” polarization is applied so that we can obtain the optimum nonlinear coefficient  $d_{33}$  of the PPLN crystal, realizing type I QPM.

In order to achieve efficient SHG, we then compared temperature phase-matching properties of the PPLN crystal and PPKTP crystal. The SHG temperature tuning curve obtained for PPKTP in experiment is shown in the Fig 4. This figure is gained by changing the crystal temperature slowly to find the optimum temperature of the best conversion efficiency at the incident fundamental power of 360 mW. There is no need to consider the temperature for PPKTP in the SH process, either. Adjusting the crystal working temperature, we can get optimum phase match.

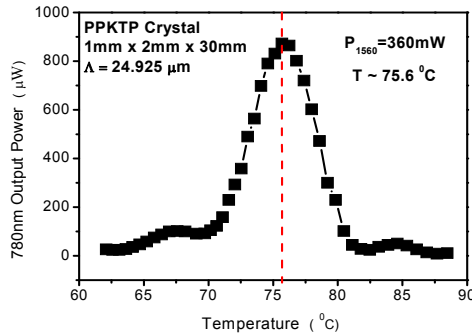


**Fig. 4** Phase-matching temperature tuning curves obtained for PPKTP

We observed that optimum matching temperature of PPKTP crystal is  $\sim 75.6^\circ\text{C}$ , while the optimum matching temperature of PPLN crystal with a period of  $18.8\mu\text{m}$  ( $19.0\mu\text{m}$ ) is  $162^\circ\text{C}$  ( $113^\circ\text{C}$ ). The difference between the experimental data and the theoretical value may be caused by the real matching periods of the crystal.

### 3.2 SHG output and SHG efficiency

Generated SH power determines the efficiency of the SHG process. In order to compare the performance of the two crystals, the power scaling measurements were performed under similar incident fundamental power, finally we increase the fundamental power to 5W, plotting the figures of the both crystals of the variation of the SH power with the fundamental power and the variation of conversion efficiency with the fundamental power. While the generated SH power was corrected for the 2% transmission loss of the DM mirror, used to separate the generated SH from the fundamental.

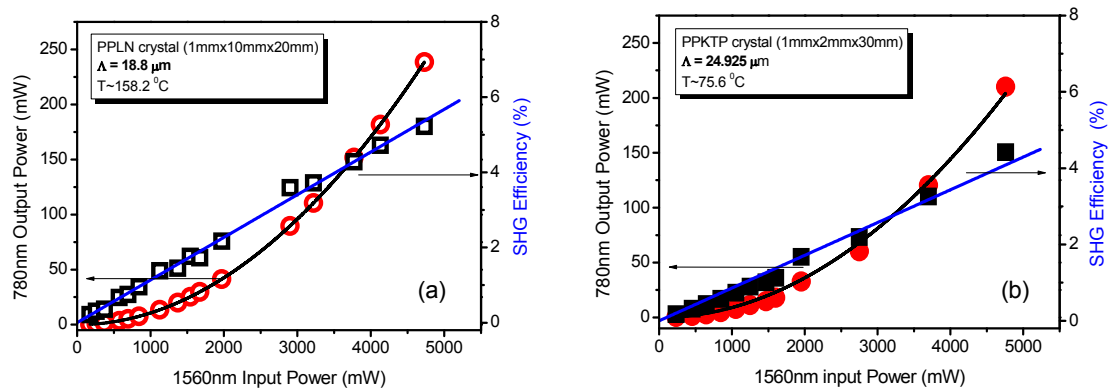


**Fig. 5** Dependence of measured SH power on the incident fundamental power for (a) PPLN and (b) PPKTP. The solid line is the theoretical curve

The results are shown in Fig. 5. Maximum power of  $\sim 239\text{mW}@780\text{nm}$  is obtained at  $\sim 5\text{ W}@1560\text{nm}$  by using of PPLN crystal, corresponding to a single-pass SHG efficiency of  $\sim 5.2\%$ ; while the maximum power is  $\sim 210\text{mW}@780\text{nm}$  obtained with PPKTP crystal at  $\sim 5\text{ W}@1560\text{nm}$ , corresponding to a single-pass SHG efficiency of  $\sim 4.4\%$ .

### 3.3 Laser frequency stabilization

Scanning the laser current we can obtain the  $D_2$  line of Rb atom, as shown in the Fig. 6. Decreasing the amplitude of the triangular signal slowly, there appears Doppler-broaden absorption spectrum corresponding to  $^{87}\text{Rb } 5S_{1/2} F_g=2 - 5P_{3/2} F_e=1,2,3$ ;  $^{85}\text{Rb } 5S_{1/2} F_g=3 - 5P_{3/2} F_e=2,3,4$ . After phase-sensitive detection via lock-in amplifier, the frequency discriminating signal can be obtained at the same time, the slope is  $128\text{ MHz/V}$ , as shown in Fig. 7(a) and (b). Decreasing amplitude of triangular wave to zero, adjusting the P and I parameters, we observed the frequency fluctuations in the free-running case and after being locked. The laser diode residue fluctuation is  $\sim \pm 3.5\text{ MHz}$  in  $30\text{ s}$ , compared with  $\sim 56\text{ MHz}$  of frequency drift in the free-running case, as shown in Fig. 8. In fact, we also monitor the frequency drift in the F-P cavity (with free spectral range  $2.5\text{ GHz}$  and fineness of  $\sim 100$ ), getting the fluctuation is  $\sim 41\text{ MHz}$  in  $30\text{ s}$ . It is lower than the data here, this may be affected by the F-P cavity's stability.

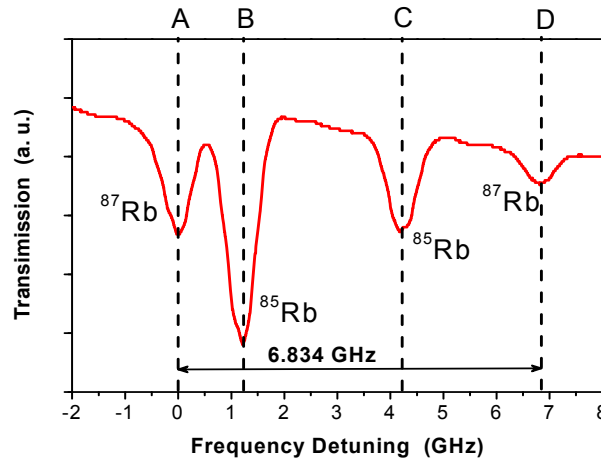


**Fig. 6** Rubidium atom Doppler-broaden absorption spectrum, A :  $^{87}\text{Rb } 5S_{1/2} F_g=2 - 5P_{3/2} F_e=1,2,3$  ; B:  $^{85}\text{Rb } 5S_{1/2} F_g=3 - 5P_{3/2} F_e=2,3,4$ ; C:  $^{85}\text{Rb } 5S_{1/2} F_g=2 - 5P_{3/2} F_e=1,2,3$ ; D:  $^{87}\text{Rb } 5S_{1/2} F_g=1 - 5P_{3/2} F_e=0,1,2$ . The scanning frequency of the triangular wave is  $14\text{ Hz}$ , the amplitude is  $\sim 110\text{ mV}$ .

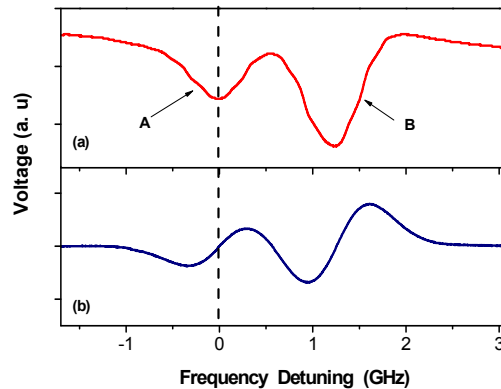


**Fig. 7** Doppler-broaden absorption spectrum (a) and corresponding frequency-discriminating signal (b). A:  $^{87}\text{Rb } 5S_{1/2} F_g=2 - 5P_{3/2} F_e=1,2,3$ ; B:  $^{85}\text{Rb } 5S_{1/2} F_g=3 - 5P_{3/2} F_e=2,3,4$ . The dashed line is the position where the laser is locked.

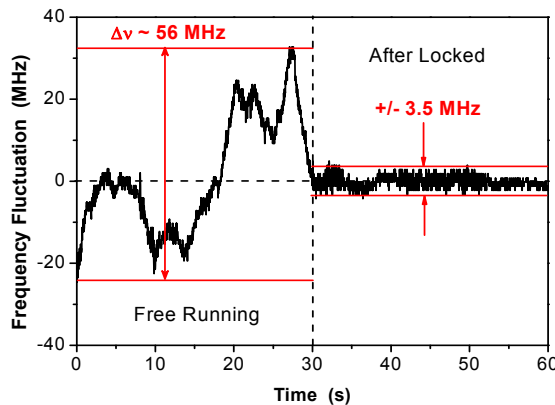


**Fig. 8** Typical laser frequency fluctuations for the free-running case and after being locked.

#### 4. CONCLUSION

In conclusion, we have demonstrated a 5W single frequency laser at 1560 nm using a diode laser seeded EDFA, and presented studies on the generation of single-frequency radiation at 780 nm using single-pass SHG in PPLN and PPKTP crystals. We demonstrated maximum SH power of  $\sim 239$  mW with a single-pass SHG efficiency of  $\sim 5.2\%$  in PPLN crystal, and  $\sim 210$  mW with a SHG efficiency of  $\sim 4.4\%$  in PPKTP. Single-pass SHG characteristics of PPLN and PPKTP crystals have been compared. Finally the 1560 nm laser diode's frequency is locked to rubidium absorption line via SHG and rubidium absorption spectrum, typical frequency drift in the free-running case is  $\sim 56$  MHz within 30 s, the residual frequency jitter after being locked is  $\sim \pm 3.5$  MHz within 30 s.

#### ACKNOWLEDGEMENT

This work is partially supported by the National Natural Science Foundation of China (Grant Nos. 61078051, 60978017, 10974125 and 60821004), the NCET Program from the Education Ministry of China (Grant No. NCET-07-0524), and the Specialized Research Fund for the Doctoral Program of China (Grant No. 20070108003).

#### REFERENCES

- [1] M. Ohtsu and E. Ikegami, "Frequency stabilization of 1.5  $\mu\text{m}$  DFB laser using internal second harmonic generation and atomic  $^{87}\text{Rb}$  line", **Electron. Lett.** 25, 22 (1989).
- [2] M. Poulin, C. Latrasse, M. Têtu, and M. Breton, "Second-harmonic generation of a 1560-nm distributed-feedback laser by use of a  $\text{KNbO}_3$  crystal for frequency locking to the  $^{87}\text{Rb}$   $D_2$  line at 780 nm", **Opt. Lett.** 19, 1183 (1994).
- [3] S. Masuda, A. Seki, and S. Niki, "Optical frequency standard by using a 1560 nm diode laser locked to saturated absorption lines of rubidium vapor", **Appl. Opt.** 46, 4780 (2007).
- [4] V. Mahal, A. Arie, M. A. Arbore, and M. M. Fejer, "Quasi-phase-matched frequency doubling in a waveguide of a 1560-nm diode laser and locking to the Rubidium  $D_2$  absorption lines", **Opt. Lett.** 21, 1217 (1996).
- [5] F. Lienhart, S. Boussen, O. Carraz, N. Zahzam, Y. Bidet, and A. Bresson, "Compact and robust laser system for rubidium laser cooling based on the frequency doubling of a fiber bench at 1560nm", **Appl. Phys. B** 89, 177 (2007).
- [6] J. F. Yang, B. D. Yang, J. Gao, T. C. Zhang, and J. M. Wang, "1560 nm cw diode laser frequency doubling by using PPLN crystal and frequency cocking via Rubidium absorption spectroscopy", **Acta Quantum Optica Sinica** 16, 41 (2010) (in Chinese).
- [7] M. M. Fejer, G. A. Magel, D. H. Jundt, and R. L. Byer, "Quasi-phase-matched second harmonic generation: tuning and tolerances", **IEEE J. Quantum Electr.** 28, 2631 (1992).
- [8] S. C. Kumar, G. K. Samanta, and M. Ebrahim-Zadeh, "High-power, single-frequency, continuous-wave second-harmonic-generation of Ytterbium fiber laser in PPKTP and  $\text{MgO:sPPLT}$ ", **Opt. Express** 17, 13711 (2009).